

5. M. Stuiver, *ibid.* 66, 273 (1961).  
 6. A. W. Fairhall and W. R. Schell, unpublished results.  
 7. The tree-ring samples from Arizona, Maine, Colorado, and Alaska were received through the courtesy of, respectively, M. A. Stokes and T. Smiley of the Laboratory of Tree-Ring Research, University of Arizona; H. E. Young of the University of Maine; E. W. Mogren of Colorado State University, and J. L. Giddings of Brown University. This research was supported by AEC under contract AT(30-1) 2652.

12 May 1965

## Germanium and Silicon

### Disulfides: Structure and Synthesis

**Abstract.** *Crystal structures of the tetragonal forms of germanium and silicon disulfide are similar and consist of  $(\text{SiS}_4)^{4-}$  and  $(\text{GeS}_4)^{4-}$  tetrahedra which share vertices to form three-dimensional networks. These tetragonal materials, synthesized at high pressure and temperature, are different from the previously known germanium and silicon disulfides.*

Silverman and Soulen have reported on the behavior of the silicon-sulfur and germanium-sulfur binaries at high pressure (1). We have studied the synthesis and structure of the tetragonal germanium disulfide and the isotypic silicon disulfide prepared by the reaction of the elements at high pressure. These tetragonal phases are apparently very similar to those found by Silverman and Soulen.

When we examined the first products of the high-pressure synthesis, we found what were apparently new phases of  $\text{GeS}_2$  and  $\text{SiS}_2$ . We could select single crystals suitable for x-ray analysis and subsequently determine the structures of both phases. These structures are similar and consist of  $(\text{GeS}_4)^{4-}$  and  $(\text{SiS}_4)^{4-}$  tetrahedra which share vertices to form three-dimensional networks. They are different from the structures of the low-pressure phases of  $\text{GeS}_2$  and  $\text{SiS}_2$  which have been known for almost 30 years. The low-pressure  $\text{SiS}_2$  (2) contains parallel chains of  $(\text{SiS}_4)^{4-}$  tetrahedra with the tetrahedra in each chain sharing edges. Low-pressure  $\text{GeS}_2$ , however, has a structure (3) in which  $(\text{GeS}_4)^{4-}$  tetrahedra share vertices. For the remainder of this paper, we shall refer to the low-pressure forms as  $\text{GeS}_2$  I and  $\text{SiS}_2$  I and to the high-pressure forms as  $\text{GeS}_2$  II and  $\text{SiS}_2$  II.

Crystals selected for analysis were of irregular shape and of the following

minimum and maximum dimensions:  $\text{GeS}_2$  II, 0.04 by 0.40 mm;  $\text{SiS}_2$  II, 0.13 by 0.50 mm. The x-ray patterns were sharp and gave no indication of twinning, disorder, or strain. The cells are tetragonal ( $Z = 4$ ), with  $a = 5.480 \pm 0.004$ ,  $c = 9.143 \pm 0.004$  Å ( $\text{GeS}_2$  II), and  $a = 5.420 \pm 0.004$ ,  $c = 8.718 \pm 0.004$  Å ( $\text{SiS}_2$  II). Measured and calculated densities for  $\text{SiS}_2$  are 2.39 and 2.37 g/cm<sup>3</sup>, respectively. The calculated density for  $\text{GeS}_2$  is 3.30 g/cm<sup>3</sup>; we had insufficient material to measure the density. Powder patterns are given in Table 1.

Silverman and Soulen (1) reported a cell for their tetragonal silicon disulfide with  $a = 5.43$  Å,  $c = 8.67$  Å, and a measured density of 2.23 g/cm<sup>3</sup>. They did not give a cell for germanium disulfide but the powder pattern, revealed by x-ray diffraction, for this phase is similar to the one given here in Table 1. Although the apparent differences in the powder pattern are probably due to variations in composition of the reaction products, the difference in densities is larger than would be expected.

The occurrence of reflections from the body-centered tetragonal  $\text{GeS}_2$  II and  $\text{SiS}_2$  II obeys the following rules:  $hkl$ ,  $h+k+l = 2n$ ;  $hh\ell$ ,  $2h+\ell = 4n$ . The diffraction symbol is  $4/mmmI$

--  $d$  which includes space groups  $I4_1md$  and  $I\bar{4}2d$ . Although both space groups are noncentrosymmetric, tests for piezoelectricity were negative.

Using chemical evidence, we selected the following trial structure in  $I\bar{4}2d$ , which later proved to be correct.

Atom	Equi-point	Symmetry	Cell coordinates
Ge or Si	4a	$\bar{4}$	0,0,0
S	8d	2	$x, \frac{1}{4}, \frac{1}{8}$

We collected three-dimensional diffraction intensities for both crystals, using an equi-inclination diffractometer with filtered  $\text{CuK}\alpha$  radiation, a scintillation detector, and pulse-height discrimination. A correction for absorption was applied in which the crystal shapes were approximated by a solid bounded by plane surfaces. While collecting the data for  $\text{SiS}_2$  II, we noted that the intensities of reference reflections were diminishing with time and that the formerly clear-white crystal was becoming cloudy, indicating that the crystal was decomposing or changing state in some way. When all reflections were checked, we found that average scale factors could be applied to each reciprocal-lattice level to adjust for this error. These data, however, are not considered to be as reliable as are those for  $\text{GeS}_2$

Table 1. X-ray patterns for  $\text{GeS}_2$  II and  $\text{SiS}_2$  II ( $I_0$ , intensity).

Index	$\text{GeS}_2$ II			$\text{SiS}_2$ II		
	Calc. (Å)	Obs. (Å)	$I_0$	Calc. (Å)	Obs. (Å)	$I_0$
101	4.70	4.72	80	4.60	4.61	75
112	2.96	2.96	100	2.88	2.88	100
200	2.74			2.71	2.71	40
103	2.66	2.66	35	2.56	2.55	20
211	2.37	2.38	45	2.34	2.34	30
004	2.29			2.18	2.17	20
220	1.94	1.94	40	1.92	1.92	60
213	1.91	1.91	30	1.86	1.85	40
301	1.79	1.80	15	1.77		
204	1.76	1.75	70	1.70	1.69	80
105	1.73	1.73	10	1.66	1.65	5
312	1.62	1.62	60	1.60	1.61	70
303	1.57	1.57	20	1.53	1.53	15

Table 2. Final atom parameters for  $\text{GeS}_2$  II and  $\text{SiS}_2$  II.

Coordinate	$\text{GeS}_2$ II		$\text{SiS}_2$ II	
	Ge	S	Si	S
$x$	0	0.2387 ± 0.0008	0	0.2272 ± 0.0004
$y$	0	.250	0	.250
$z$	0	.125	0	.125
$B^*$	0.62	.51	0.72 ± 0.16	1.31 ± 0.16
$\beta_{11}$	0.0057 ± 0.0007	0.0053 ± 0.0008		
$\beta_{22}$	0.0057	0.0033 ± 0.0008		
$\beta_{33}$	0.0015 ± 0.0005	0.0015 ± 0.0005		
$\beta_{12}$	0	0		
$\beta_{23}$	0	0.0011 ± 0.0007		
$\beta_{13}$	0	0		

\* The isotropic  $B^*$ 's for  $\text{GeS}_2$  are the equivalents computed from the anisotropic values.

II. X-ray photographs taken several months after the intensities were collected showed no diffraction spots and only diffuse rings, indicating that the crystal had been completely altered. Since the crystal was exposed to the atmosphere, it may have been hydrolyzing. There was no indication of a transformation to  $\text{SiS}_2$  I or to any other crystalline phase.

Refinement of both sets of data resulted in overall  $R$  factors [ $R = \sum ||F_o| - |F_c|| / \sum |F_o|$ ] of 0.059 for  $\text{GeS}_2$  II and 0.120 for  $\text{SiS}_2$  II. Although the temperature factors of Ge and S were refined anisotropically for the former compound, we felt that the data did not warrant anisotropic refinement for  $\text{SiS}_2$  II, even though the isotropic  $B$ 's for Si and S in  $\text{SiS}_2$  II are possibly more reasonable than the  $B$ 's for Ge and S in  $\text{GeS}_2$  II. Results of least-squares refinement are given in Table 2.

Figure 1 depicts the crystal structure of these compounds. In this structure, the  $x$  coordinate for S is the only positional variable. If this variable were zero and the tetrahedra regular, the structure would correspond to that of the Wyckoff (4) high cristobalite ( $\text{SiO}_2$ ) in which tetrahedra share vertices and form a network with Si-O-Si angles of  $180^\circ$  [although Barth (5) later proposed that these angles depart somewhat from  $180^\circ$ ]. The results of least-squares refinement show, however, that the  $\text{GeS}_2$  II and  $\text{SiS}_2$  II structure is considerably different from that of high cristobalite and also from that of low cristobalite which has also been refined (6). Instead, it is more like the tetragonal  $\text{BPO}_4$  ( $\text{BaSO}_4$ ) structure (7).

First-coordination interatomic distances in  $\text{GeS}_2$  II and  $\text{SiS}_2$  II, shown in Table 3, are comparable to those of  $\text{GeS}_2$  I and  $\text{SiS}_2$  I. The main differences are in the second- and greater-coordination distances because the high-pressure structures are much more compact. The coordination polyhedra in the high-pressure structures are actually tetragonal bisphe-noids rather than tetrahedra. Foreshortening of the bisphe-noids along the  $\bar{4}$  axes results in two long S-S vectors normal to the  $\bar{4}$  axes and four shorter vectors along the other edges of the bisphe-noids. A notable point is that the Ge-S-Ge and Si-S-Si angles are nearly tetrahedral, thus showing the essential difference between this and the cristobalite structures.

It is appropriate to mention here the work of Dachille and Roy (8) on the

Table 3. Interatomic distances (in angstroms) and interbond angles.

Distance or angle	$\text{GeS}_2$ II	$\text{SiS}_2$ II
M-S (4)	2.21 <sub>2</sub>	2.13 <sub>0</sub>
S-S (2)	3.78 <sub>8</sub>	3.66 <sub>0</sub>
S-S' (4)	3.52 <sub>6</sub>	3.38 <sub>4</sub>
M-M	3.56 <sub>8</sub>	3.47 <sub>8</sub>
S-M-S	117.8 <sup>o</sup>	118.5 <sup>o</sup>
S-M-S'	105.5 <sup>o</sup>	105.2 <sup>o</sup>
M-S-M'	107.5 <sup>o</sup>	109.4 <sup>o</sup>

effect of pressure on  $\text{BaSO}_4$  and  $\text{BPO}_4$ . These compounds, whose low-pressure phases are analogous to our disulfides, transform at about 35 and 45 kb, respectively, to the quartz structure. It is possible that the disulfides would also undergo a change to the quartz structure under higher pressure. However, since the essential difference between the disulfide structures and cristobalite is in the apparent requirement for tetrahedral M-S-M angles in the disulfides, this may also influence the formation of a higher-pressure disulfide phase since the Si-O-Si angle in  $\alpha$ -quartz is about  $144^\circ$ . Whether these features can be compatible has not been determined.

The syntheses were effected in a tetragonal anvil press of National Bureau of Standards design (9). The pressure was calibrated on the basis of the electrical transitions for Bi (25.4 kb and 26.9 kb), Tl (36.7 kb), and Ba (59.0 kb) (9). Temperatures were measured with platinum-rhodium thermocouples uncorrected for pressure effects. The thermocouples were adjacent to the graphite heaters. To minimize contamination and oxidizing side

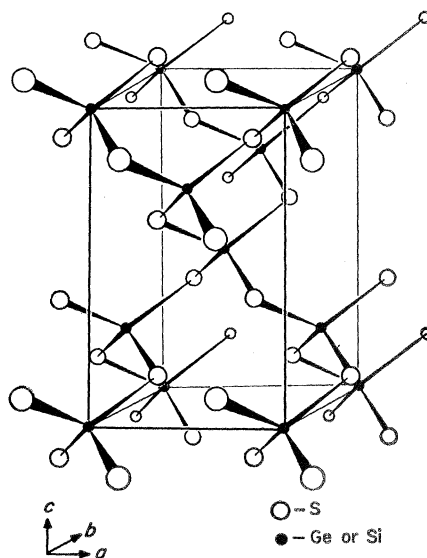


Fig. 1. Structure model for  $\text{GeS}_2$  II and  $\text{SiS}_2$  II.

reactions, all syntheses were carried out in boron nitride containers inserted in pyrophyllite tetrahedra.

For a typical synthesis of tetragonal silicon disulfide, a mixture of silicon (99.99+ percent) and sulfur, in an atom/1 : 2 ratio, compacted in a boron nitride crucible, was subjected to 60 to 65 kb at room temperature. During subsequent heating to  $1300^\circ\text{C}$  over about an hour, an exothermic reaction occurred at 875 to  $900^\circ\text{C}$ . The reaction temperature of  $1300^\circ\text{C}$  was maintained for 2 hours followed by cooling at  $150^\circ\text{C}$  per hour to around  $600^\circ\text{C}$  and quenching. Products prepared in this manner were entirely crystalline and gave powder patterns as shown in Table 1. Numerous crystals suitable for single-crystal studies were available from the columnar growth observed at both ends of the boron nitride container.

Satisfactory crystals of tetragonal germanium disulfide were similarly prepared by using germanium (99.99+ percent) and sulfur in stoichiometric ratio. The preparation was held at  $1100^\circ\text{C}$  and 60 to 65 kb for 2 to 3 hours and quenched to a totally crystalline product. The germanium disulfide could also be prepared at 30 kb and  $900^\circ\text{C}$ . The isostructural silicon disulfide was not formed at 30 kb and  $800^\circ\text{C}$ , and only a portion of the elemental reactants were converted at 40 to 42 kb and  $800^\circ\text{C}$  over a 5-hour period at temperature.

The question of isomorphous substitution in the tetragonal structure was explored by reactions of the elements with cation ratios in the range of 1 : 3 to 3 : 1. A pressure of 60 to 65 kb was applied and then the temperature was raised to  $1300^\circ\text{C}$  and held for 3 hours. Reactions were quenched after cooling at  $150^\circ\text{C}$  per hour to  $600^\circ\text{C}$ . Such products also were totally crystalline, and when analyzed by x-ray diffraction gave powder patterns comparable to those of the tetragonal end-members. Photographs obtained by the precession method (10) showed that, although these products were apparently of single phase, individual grains were not single crystals, but were aggregates of crystallites roughly aligned in the same way. There was no evidence of Si/Ge ordering in any of the photographs. Cell sizes in each case were intermediate to those of the end members.

Early observations of products from the reactions of silicon and germanium with sulfur disclosed birefringence in

the transparent crystals. With larger crystal fragments of SiS<sub>2</sub> II, uniaxial interference figures were observed in agreement with the tetragonal structure. In general, crystal fragments were colorless.

With sulfur-selenium melts of different compositions, the immersion method indicated mean indices of refraction for SiS<sub>2</sub> II and GeS<sub>2</sub> II of 2.24 and 2.40, respectively.

All crystals of SiS<sub>2</sub> II, GeS<sub>2</sub> II, and mixed compositions essentially behaved as insulators having electrical resistivities in excess of 10<sup>10</sup> to 10<sup>11</sup> ohm cm.

C. T. PREWITT

H. S. YOUNG

Central Research Department,  
Experimental Station, E. I. du Pont  
de Nemours and Company,  
Wilmington, Delaware 19898

#### References and Notes

1. M. S. Silverman and J. R. Soulen, *Inorg. Chem.* **4**, 129 (1965).
2. W. Büssem, H. Fischer, E. Gruner, *Naturwissenschaften* **23**, 740 (1935); E. Zintl and K. Loosen, *Z. Physik. Chem. Leipzig A* **174**, 301 (1935).
3. W. H. Zachariasen, *Phys. Rev.* **49**, 884 (1936); *J. Chem. Phys.* **4**, 618 (1936).
4. R. W. G. Wyckoff, *Am. J. Sci.* **9**, 448 (1925); *Z. Krist.* **62**, 189 (1925).
5. T. F. W. Barth, *Am. J. Sci.* **23**, 350 (1932).
6. W. A. Dollase, *Z. Krist.*, in press.
7. G. E. R. Schulze, *Z. Physik. Chem. Leipzig B* **24**, 215 (1934).
8. F. Dacheille and R. Roy, *Z. Krist.* **111**, 451 (1959).
9. E. C. Lloyd, U. O. Hutton, D. P. Johnson, *J. Res. Nat. Bur. Std. C* **63**, 59 (1959).
10. S. Block, C. W. Weir, G. J. Piermarini, *Science* **148**, 947 (1965).
11. We acknowledge with thanks the efforts of C. L. Hoover and his staff who carried out the pressure syntheses, the efforts of H. G. Hoeve who measured the indices of refraction, and the assistance of E. P. Moore with the x-ray work. Contribution No. 1081 from the Central Research Department, Experimental Station, E. I. du Pont de Nemours and Company.

1 June 1965

lyzed. It was then possible to make a direct comparison between the amounts of Po<sup>210</sup> and particulate matter in mainstream smoke. Eleven popular brands of cigarettes were tested. These included one regular-sized nonfilter, one regular-sized filter, and one king-sized nonfilter cigarette, and eight king-sized filter cigarettes. Cigarettes were purchased on the open market and used from freshly opened packs. They were smoked to approximately equal butt lengths, which required fewer puffs for regular-sized than for king-sized cigarettes.

The particulate phase of mainstream smoke was trapped on Millipore type AP fiberglass prefilter discs held in a modified Unico filter-disc holder with reduced dead space. Efficiency of the filter was checked in the following manner. Smoke from test cigarettes was passed first through a fiberglass filter and then through a Millipore filter—type HA, of 0.45- $\mu$  pore-size—which is assumed to act as an absolute filter for smoke particles. When both filters were weighed separately, it was found that a minimum of 96 percent of the particulate phase was retained by the fiberglass filter. Cigarettes held by a latex diaphragm cemented to a small glass funnel were smoked in a horizontal position. The latex diaphragm provides a leak-proof, distortion-free method for holding cigarettes and does not affect smoke flow. A falling-water-column apparatus provided suction standardized in 35-ml puffs of 2-second duration at 58-second intervals. The criteria for puff frequency, duration, and size are those set forth by

## Polonium-210 Content of Mainstream Cigarette Smoke

**Abstract.** *When eleven brands of cigarettes were smoked in a standardized manner, differences in the polonium-210 content of various brands were found. The differences were not directly related to the presence of a filter or to the construction of the filter, but were related to the amount of particulate matter in the mainstream smoke.*

Polonium-210, a radioisotope that emits  $\alpha$ -particles, is a natural contaminant of cigarette smoke. Radford and Hunt (1) suggested that Po<sup>210</sup> is an important factor in the genesis of bronchial cancer in smokers. These authors measured the Po<sup>210</sup> content of cigarette smoke, whole tobacco, and samples of bronchial tissue. The validity of their conclusions regarding both the quantities of Po<sup>210</sup> found in the lung and the importance of the role of Po<sup>210</sup> in tumor initiation has been discussed (2, 3). Radford and Hunt's data further revealed a marked difference between the Po<sup>210</sup> content of mainstream smoke from filter and nonfilter cigarettes. Michelson (2) pointed out that the difference was substantial and might be related to the action of cigarette filters in removing portions of the particulate phase of the smoke. It has also been suggested that Po<sup>210</sup> might explain the increased incidence of bladder cancer in smokers (4).

Because Po<sup>210</sup> may be a significant factor in the initiation of bronchial cancer in smokers, it is important to have more accurate and extensive information about the quantities of Po<sup>210</sup> in mainstream smoke. Furthermore, if there are real differences in

the Po<sup>210</sup> content of smoke among cigarette brands, they would probably be due to the action of cigarette filters. The characteristic of cigarette filters which makes them effective against Po<sup>210</sup> should also be investigated.

To resolve these questions, cigarettes were smoked in a standardized manner, the particulate phase removed and measured, and the Po<sup>210</sup> content ana-

Table 1. The Po<sup>210</sup> content of mainstream smoke of various brands of cigarettes. For each analysis two cigarettes were used. Except where indicated, nine puffs were used for each cigarette.

Brand	No. of analyses	Average butt length (mm)	Range	Radioactivity of mainstream smoke per cigarette (pc)
A	9	<i>Regular-sized filter cigarette</i>		.029 $\pm$ .0023*†
		32.2	(30-34)	
B	5	<i>Regular-sized nonfilter cigarette</i>		.043 $\pm$ .0032†
		30.9	(29-32)	
C	9	<i>King-sized filter cigarette</i>		.029 $\pm$ .0020
		32.1	(31-33)	
		32.4	(31-34)	
		34.4	(30-36)	
		34.3	(33-35)	
		32.2	(31-34)	
		35.4	(34-37)	
		34.0	(32-36)	
J	6	<i>King-sized nonfilter cigarette</i>		.042 $\pm$ .0021
K	6	<i>King-sized filter cigarette</i>		.044 $\pm$ .0033
		34.3	(33-35)	

\* Plus or minus standard error. † Six puffs for each cigarette. ‡ The average number of puffs was 9.25; the range was nine to ten.